

Analyst

Accepted Manuscript



This is an *Accepted Manuscript*, which has been through the Royal Society of Chemistry peer review process and has been accepted for publication.

Accepted Manuscripts are published online shortly after acceptance, before technical editing, formatting and proof reading. Using this free service, authors can make their results available to the community, in citable form, before we publish the edited article. We will replace this *Accepted Manuscript* with the edited and formatted *Advance Article* as soon as it is available.

You can find more information about *Accepted Manuscripts* in the [Information for Authors](#).

Please note that technical editing may introduce minor changes to the text and/or graphics, which may alter content. The journal's standard [Terms & Conditions](#) and the [Ethical guidelines](#) still apply. In no event shall the Royal Society of Chemistry be held responsible for any errors or omissions in this *Accepted Manuscript* or any consequences arising from the use of any information it contains.

ANALYST

CRITICAL REVIEW

NMR-based dynamics of free glycosaminoglycans in solution**Vitor H. Pomin^{*1}**

^{*}Program of Glycobiology, Institute of Medical Biochemistry Leopoldo de Meis, and University Hospital Clementino Fraga Filho, Federal University of Rio de Janeiro, Rio de Janeiro, RJ, 21941-913, Brazil.

Running head-title: Solution NMR dynamics of free glycosaminoglycans

Keywords: chondroitin sulfate; heparan sulfate; heparin; hyaluronan; molecular dynamics; N-acetyl hexosamine; NOE; scalar coupling; spin relaxation

¹To whom correspondence should be addressed: R. Prof. Rodolpho Paulo Rocco, 255, HUCFF 4A01, Ilha do Fundão, Rio de Janeiro, RJ, 21941-913, Brazil. Tel. +55-21-3938-2939; Fax: +55-21-3938-2090; e-mail: pominvh@bioqmed.ufrj.br.

1
2
3 ABSTRACT

4 Glycosaminoglycans (GAGs) comprise a special class of complex carbohydrates endowed with
5 numerous biological functions. Most of these functions are regulated by conformational
6 arrangements or dynamical properties of GAGs in solution. Nuclear magnetic resonance (NMR)
7 is a powerful technique used for dynamic analyses. Spin relaxation, scalar couplings, chemical
8 shifts and nuclear Overhauser effect resonances are the commonest NMR parameters utilized in
9 such analyses. Computational molecular dynamics are also very often employed in conjunction
10 with, or restrained by, the NMR dataset. This report aims at describing the major NMR-based
11 information available so far concerning the dynamical properties of free GAGs in solution.
12
13
14
15
16
17
18
19
20
21
22
23
24
25
26
27
28
29
30
31
32
33
34
35
36
37
38
39
40
41
42
43
44
45
46
47
48
49
50
51
52
53
54
55
56
57
58
59
60

1. INTRODUCTION

1.1 Glycosaminoglycan families and structures

Glycosaminoglycans (GAGs) are sulfated polysaccharides composed of disaccharide building blocks formed by alternating hexosamine and uronic acid units. The GAG families are heparin, heparan sulfate, chondroitin sulfate, dermatan sulfate, keratan sulfate and hyaluronic acid also known as hyaluronan. These families are classified based on the structural patterns. Heparin, heparan sulfate, chondroitin sulfate and hyaluronan are the GAG families mostly studied by NMR dynamics. Hence, we will be discussing only these three GAG families in this report. Heparin and heparan sulfate share basically the same backbone type composed of 4-linked *N*-acetyl glucosamine (GlcNAc) and 4-linked glucuronic acid (GlcA)^{1,2} (Fig. 1). The heparin chain is highly processed during its biosynthesis through epimerization and sulfation processes. This gives rise to a very heterogeneous structure composed of a combination of the epimerized iduronic acid (IdoA), the unepimerized GlcA, together with 6-sulfated GlcNAc (GlcNAc6S), 6-sulfated *N*-sulfated glucosamine (GlcNS6S).³ In heparin, the IdoA unit can also be sulfated at 2-position (IdoA2S)³ (Fig. 1). Although these units are present in heparan sulfate chains, they are found at much lower concentrations in this GAG type. This makes heparan sulfate a less heterogeneous polysaccharide. Chondroitin sulfate chains are composed of 3-linked *N*-acetyl galactosamine (GalNAc) and 4-linked GlcA (Fig. 1). It can be sulfated at positions 4 and 6 of the GalNAc unit.⁴ Hyaluronan is the only non-sulfated GAG. It is composed of 3-linked GlcNAc and 4-linked GlcA units⁵ (Fig. 1).

1.2 GAG functions determined by dynamical properties

Certain biological actions of GAGs are directly regulated by their dynamical behaviors or conformational oscillations. This is clearly seen by comparing the overall conformational changes of GAG molecules, or the specific conformational changes of their composing units, upon binding with functional proteins versus the unbound states in solution. For instance, while the composing GlcA and glucosamine (GlcNX) units in heparin/heparan sulfate adopt mostly the ⁴C₁ chair conformation (Fig. 2) in solution, regardless substitution patterns, IdoA units, either 2-sulfated or not, are conversely way more flexible because they have the ability to undergo ring conformational changes. Two chairs (⁴C₁ and ¹C₄) and one skew-boat (²S₀) conformations (Fig. 2) can be seen for IdoA rings in aqueous solution.⁶ The percentage of these IdoA ring conformers changes according to solvents, substitutions, polymerization degrees, adjacent units, and primarily in the presence and type of GAG-binding proteins.⁶ There is a great consensus that upon binding with several functional proteins such as fibroblast growth factor-2 (FGF-2), fibroblast growth factor-2 receptor (FGFR2), antithrombin (AT), and eosinophil cationic protein (ECP), regardless the different functions and structures of these proteins, a selection or induction of the ²S₀ skew-boat conformation of IdoA2S unit (to almost 100% of the total population) will

1
2
3 occur.⁷⁻¹⁰ This means that the protein-bound states of heparin, and likely heparan sulfate, will
4 selectively stabilize the 2S_0 ring conformation of the composing IdoA2S units to its 2S_0 skew-
5 boat shape. This explains why heparin or the IdoA2S-rich sequences of heparan sulfate are
6 biologically active. They just contain the monosaccharide type which is able to undergo
7 conformational changes that allow the proper interaction with functional proteins. With the
8 protein examples taken above, we could infer that dynamic properties of heparin, and heparan
9 sulfate, are therefore regulating biological functions like angiogenesis (via interactions with
10 FGF-2, and FGFR2), coagulation/thrombosis (via interaction with AT), and inflammatory
11 responses (via interaction with ECP).
12
13
14
15
16

17 **1.3 The commonest NMR parameters utilized in dynamic analysis**

18
19
20 The commonest parameters utilized in NMR dynamic studies of GAGs are spin relaxation, and
21 changes on chemical shift and scalar coupling values. Nuclear Overhauser effect (NOE)
22 resonances are also usually employed, especially in conjunction with computational calculations.
23
24

25 **1.3.1 Spin relaxation.** The two types of spin relaxation phenomena are the lattice (also
26 known as the longitudinal) relaxation, and the spin-spin (also named transverse) relaxation.⁶ The
27 time course of the former is designated as T_1 , and its ratio ($1/T_1$) is known as R_1 . The relaxation
28 time for the latter is known as T_2 , and its ratio ($1/T_2$) is known as R_2 . The dynamic-dependent
29 spin-spin relaxation T_2 influences the resultant linewidths of the resultant resonances in the NMR
30 spectrum. Both spin relaxation times (T_1 and T_2) as well as linewidths are dependent on the
31 overall or punctual molecular motions. In general, the faster these motions lower T_1 values,
32 higher T_2 values, and sharper the lines (thinner linewidths). The spin relaxation values can be
33 obtained by specific NMR experiments such as the inversion recovery for T_1 measurements, and
34 the Carr-Purcell-Meiboom-Gill (CPMG) experiment and Lorentzian linewidth measurements for
35 T_2 assessment. The principles involved in these experiments can be understood from other
36 publications.¹¹⁻¹³
37
38
39
40
41
42

43 **1.3.2 Changes on chemical shift values.** Theoretically speaking, chemical shift (δ) could be
44 defined as the resonance frequency of a given nucleus related to a specific standard frequency,
45 both under the application of the same external magnetic field, usually named B_0 . The resultant
46 chemical shift values seen in a NMR spectrum are B_0 -independent because they are always
47 referenced to the standard, and the difference between the frequencies of the observed nuclei and
48 the standard changes equally proportional to the applied B_0 . Conversely and fortunately,
49 chemical shifts are directly dependent of the chemical environment of the observed nucleus
50 within the molecules of the sample targeted to analysis. This aspect is extremely important since
51 it will ultimately lead to the resultant multiple lines in the NMR spectrum. Therefore, chemical
52 shifts are characteristic of the local chemical environment of a given nucleus. This environment
53 may be assumed as a final result of many structural aspects that surround the nucleus. The
54
55
56
57
58
59
60

1
2
3 principal structural aspects are the local interactions such as through-bond, through-space
4 contacts with other nuclei that are located nearby, and the local environment fluctuations such as
5 oscillations caused by dynamics and interchanging conformational states that are experimented
6 by the observed nucleus during the NMR experiment. This information explains why chemical
7 shifts are sensitive to temperature, pH, and primarily to the conformational states adopted by the
8 molecules in solution. Based on this, if a certain molecule, like GAGs, experience
9 conformational fluctuations as a result of different experimental conditions or natural behavior in
10 solution, the chemical shift values will change (downfield if the frequency rises, or upfield if the
11 frequency decreases). This change in chemical shift values is indicative of dynamical process,
12 and then, can be successfully employed in NMR dynamic studies of the molecules in solution.^{6,}
13
14
15
16
17

18
19
20 **1.3.3 Changes on scalar coupling values.** Besides chemical shifts, scalar coupling constants
21 are also very useful NMR parameters utilized for assessing molecular conformational states as
22 well their motions in solution. Theoretically speaking, scalar couplings, also known as spin-spin
23 couplings are NMR-based structural information essentially originated from a through-bond
24 correlation. This type of information is generated because, during a NMR experiment, the
25 magnetizations of long- and mostly short-distanced nuclei have the capacity to influence
26 chemical shifts of each other nuclei within the molecule, resulting thus splitting resonances in the
27 spectrum. The influential nuclei with splitting resonances are named coupled. The distance
28 between the frequencies (or chemical shifts) of the resultant splittings from the coupled nuclei
29 are the coupling constants. Coupling constants (frequently measured in Hz) are values usually
30 denoted by the letter *J*. Between protons it will be denoted J_{H-H} ; between ^{13}C nuclei it will be J_{C-}
31 c ; between protons and deuterions it will be J_{D-H} , and so forth. The number of bonds between the
32 coupled nuclei is indicated by a superscript preceding the *J*. Hence 1J denotes a coupling
33 between directly bonded nuclei, 2J means a germinal coupling, 3J means a vicinal coupling, and
34 ^{3+n}J a long-range coupling. The factors that influence the coupling constants are the following:
35 (i) the hybridization of the atoms involved in the coupling; (ii) bond angles and torsion angles of
36 the coupled nuclei; (iii) lengths of both coupled nuclei; (iv) the presence of neighboring π -bonds;
37 (v) effects of neighboring electron lone-pairs; and (vi) substitutes effects. Like chemical shifts,
38 scalar coupling constant values are also quite informative of conformational states and motion of
39 molecules in solution. Their changes at different experimental conditions, which in turn represent
40 different conformational possibilities, are useful indicatives of dynamical process, and then, can
41 be successfully employed in NMR dynamic studies of the molecules in solution.⁶
42
43
44
45
46
47
48
49
50

51 **1.4 The combination of NMR and computational molecular dynamics.**

52

53
54 Molecular dynamics (MD) relies on computational calculations of the molecules subjected to
55 virtual simulations in which a series of parameters might be used as input in the computational
56 program to derive structural restraints.^{15,16} Besides the MD virtual parameters, sometimes NMR-
57
58
59
60

1
2
3 derived information can be also used as additional input parameters, and thus NMR-restrained
4 MD data can be generated. In these cases, a perfect match between experimental and theoretical
5 data is achieved, and consequently, a more reliable set of information is provided. MD combined
6 with NMR usually provides distances, usually in angstroms, between spatially closed atomic
7 nuclei. This type of information is usually obtained by NOE resonances from NMR experiments
8 named NOESY, for nuclear Overhauser effect spectroscopy. The NOE signals are measurements
9 of through-space contact distances of inter-nuclei. The dihedral angles as well as their changes
10 according to dynamical processes are features examined by MD analysis. Changes in dihedral
11 angle values imply molecular motions. The dihedral angles can be experimentally obtained by
12 NMR analysis of the scalar coupling constant values of vicinal proton-proton pairs ($\underline{\text{H}}\text{-C-C-}\underline{\text{H}}$) as
13 well as of those involved in the interglycosidic bonds ($\underline{\text{H}}1\text{-C1-O1-CX-}\underline{\text{H}}\text{X}$). The latter is relevant
14 to understand the motions involved in tow or more residues within a chain. The dihedral angles
15 can be applied into Karplus relationships^{17,18} to allow measurements of the distributions of
16 conformers in solution as well as to determined the changes in these conformer populations as a
17 function of dynamics.
18
19
20
21
22
23
24
25
26

27 **2. NMR-BASED DYNAMICS OF HEPARIN AND HEPARAN SULFATE: THE ROLE** 28 **OF IDOA UNITS, SULFATION PATTERNS, AND EXPERIMENTAL CONDITIONS**

29
30
31 Since the structures of heparin and heparan sulfate are basically composed of the same
32 monosaccharide building blocks although within different amounts^{1,2} (Fig. 1), it sounds
33 reasonable here to discuss the NMR-dynamical properties of these two GAG types together at
34 the same section.
35
36

37 **2.1 Polysaccharides**

38
39
40 As mentioned earlier at section 1.2, IdoA units have the ability to undergo conformational
41 changes in solution or upon physicochemical variations such as solvents, temperatures, ions and
42 in the presence of certain GAG-binding proteins. Hence, there was a general belief that IdoA-
43 containing sequences in heparin/heparan sulfate should be flexible regions of these molecules.
44 However, Mulloy and Foster have shown that although the IdoA units, and in analogy the IdoA-
45 composed sequences, can freely interconvert in solution, the overall conformational shapes of
46 heparin and heparan sulfate are not significantly altered as a function of the ¹C₄ chair and the ²S₀
47 skew-boat conformations of the composing IdoA.¹⁹ This implies that, even though IdoA means a
48 dynamic spot in heparin/heparan sulfate, the conformational variations of these molecules is
49 somewhat stabilized by other structural features. This conclusion comes from a combination of
50 NMR (¹³C *T*₁ and *T*₂ relaxation and NOE) and MD studies on heparin and heparan sulfate.¹⁹
51
52
53
54

55 Indeed, Mobli and coworkers have shown, based on ¹⁵N *T*₁ relaxation and NOE studies
56 that *N*-sulfation-rich domains (also known as NS domains) has limited mobility when compared
57
58
59
60

1
2
3 to the *N*-acetylation-rich domains (also known as NA domains) of heparin/heparan sulfate.²⁰ T_1
4 measurements of the amides of acetamido-composed HS oligosaccharides (*N*-acetylated
5 oligosaccharides that represent the NA domains) has dynamic properties on the NMR timescale
6 of a few seconds to several hundreds of milliseconds. In comparison with the data from
7 sulfamate-composed HS oligosaccharides, which represent the NS domains, the relaxation data
8 obtained is in the order of nanosecond timescale. This implies that *N*-sulfation is a dynamic
9 barrier that restricts considerably the flexibility of heparin and heparan sulfate in solution. This
10 explains why heparin is more structurally rigid than heparan sulfate in solution, despite the
11 higher abundance of IdoA (the flexible monosaccharide). Mobli and co-authors have raised the
12 hypothesis that NS domains (and likely heparin which is mostly composed of NS sequences) are
13 more capable of protein interactions than the NA domains (and likely heparan sulfate which is
14 mostly composed of the NA sequences). This happens because of the less dynamic behavior or
15 more structured nature of NS domains (and heparin) in solution, besides the higher
16 electronegative property of the NS domains. The authors consider the NS domains protein-
17 interacting paths, while the NA domains are paths of less protein binding potentials, although
18 highly functional in terms to maintain the dynamic character of the heparin and heparan sulfate
19 chains in solution.²⁰ The NA/NS domains would show properties of these two domains
20 combined.
21
22
23
24
25
26
27
28

29 2.2 Oligosaccharides and disaccharides

30
31 Information regarding NMR-based dynamical properties of heparin- and heparan sulfate-derived
32 oligosaccharides exist in the literature for the heparin pentasaccharide of high-affinity for AT,²¹
33 heparin-like hexasaccharides,²² heparan sulfate hexasaccharides,²³ and heparin disaccharides.²⁴
34 These works are based on NOE,^{21,22} ^{13}C T_1 and T_2 relaxation measurements,^{21,22} scalar coupling
35 values,^{23,24} chemical shift values,²³ and MD simulations.^{23,24}
36
37
38

39 The synthetic AT high-affinity heparin pentasaccharide showed a very complex motional
40 behavior in solution.²¹ Both overall and internal motions have been noted for this heparin
41 oligosaccharide. The rate of internal motions is on a picosecond timescale, and that order
42 parameter decreases from the central residue towards both ends of the oligosaccharide. The
43 analysis has also shown that the order parameters differ from various relaxation vectors,
44 depending on the orientational perspective within the pentasaccharide as a consequence of
45 anisotropic motions and tumbling. The anisotropic motions are characteristic of non-spherical
46 models. The anisotropic dynamic behavior of the AT high-affinity heparin pentasaccharide was
47 confirmed with their significant rates of chemical shift anisotropy relaxation mechanisms
48 measured in the reference work.²¹ Therefore, different internal motions of the heparin
49 pentasaccharide associated with the anisotropic tumbling collaborates together to the complex
50 dynamic nature of this GAG oligosaccharide in solution.²¹
51
52
53
54

55 The dynamic properties of two biologically active synthetic heparin-like hexasaccharides
56 were examined in terms of their heteronuclear NOE and ^{13}C T_1 and T_2 relaxation properties at
57 several magnetic fields (500 , 600 and 800 MHz for proton Larmor frequency).²² These heparin
58
59
60

1
2
3
4
5
6
7
8
9
10
11
12
13
14
15
16
17
18
19
20
21
22
23
24
25
26
27
28
29
30
31
32
33
34
35
36
37
38
39
40
41
42
43
44
45
46
47
48
49
50
51
52
53
54
55
56
57
58
59
60

hexasaccharides differ only in terms of sulfation patterns, and they are able to induce fibroblast growth factor-1 (FGF-1)-dependent mitogenesis. The data have indicated that, like the heparin pentasaccharide,²¹ both hexasaccharides exhibit remarkable anisotropic overall motions in solution.²² Fast internal motions were also observed, specially at the less sulfated compound. This supports the conception that sulfation is a restricting feature for dynamics of heparin and derivatives.

NMR characterization of two heparan sulfate hexasaccharides derived from porcine mucosa obtained by enzymatic depolymerization, gel filtration and strong anion exchange chromatographies, has enabled measurements of internal IdoA coupling constants under the influence of different flanking sequences.²³ After fitting the experimental scalar coupling constant data to a set of theoretical coupling constant values, calculated using explicit water MD simulations, the investigators were able to offer new insights into the role of sequences and sulfation patterns over influencing IdoA conformational and dynamical properties. The data have suggested that replacement of the *N*-sulfate group to the reducing side of the IdoA unit by *N*-acetyl group has little effect on the balance of the IdoA ring conformational equilibrium. However, fitting the coupling constants from sequences GlcNS-IdoA2S-GlcNS and GlcNS6S-IdoA2S-GlcNS suggested that the flanking 6-*O*-sulfonation has the meaning capacity to considerably alter the balance of the IdoA2S conformational equilibrium, more toward the ²S₀ skew-boat conformation (Fig. 2). The authors have also seen a cooperative effect between *N*- and 6-sulfation. But, their conclusion have clearly indicated the regulatory function of 6-sulfation in conformational flexibility of IdoA-containing sequences in heparan sulfate chains, and in analogy, in heparin chains as well. The conclusions from reference²³ go in favor with the findings from Mulloy and Foster¹⁹, and Mulloy and co-authors^{25,26} about the effects of sulfation patterns on the structural conformations and dynamic properties of heparin and heparan sulfate. Murphy and coworkers have just improved this explanation, adding that 6-sulfation, in cooperation with *N*-sulfation, has the effect to shift the equilibrium of the IdoA ring conformation toward a selective conformational equilibrium.²³ In synthesis, the conformational changes in heparin and heparan sulfate, which are controlled ultimately by the IdoA dynamic behavior, are primarily regulated by sulfation patterns (Fig. 3)^{25,26}, especially 6-sulfation combined with *N*-sulfation.²³ Hence, sulfation patterns are the main cause of conformational and dynamical properties in heparin and heparan sulfate chains in solution, rather than primarily by the IdoA flexibility.

Besides sulfation patterns and the varying IdoA ring conformations, which are both intrinsic regulatory aspects of the conformational and dynamical properties of heparin and heparan sulfate, certain extrinsic aspects such as solvents, counterions and temperatures are also influential to the process. In order to examine the contribution of solvent effect and counterions on the conformations and dynamics of heparin, Hricovíni examined the experimental and theoretical (obtained by computational MD calculations) proton-proton and proton-carbon scalar coupling constants of heparin disaccharides influenced by different counterions, such as Na⁺ and Ca²⁺.²⁴ Hricovíni also compared the solvent-caused coupling constant variations with the non-

1
2
3 solvated model. Solvent effects were treated by using explicit water molecules in MD
4 simulations. His data have indicated that solvent has little influence upon the magnitude of the
5 proton-proton spin-spin coupling constants. Based on inter-atomic distances, bond and torsion
6 angles, the data have indicated that in heparin disaccharide structures, the 2-sulfation of IdoA
7 units and *N*,6-di-sulfation of adjacent GlcNX units are influential to the geometry of each
8 monosaccharide. This conclusion goes again in favor that sulfation patterns are the ultimate
9 regulators of the structures and dynamics of heparin (and likely heparan sulfate) in solution.
10 Moreover, Hricovíni has also observed, by examining optimized heparin disaccharide
11 geometries, that counterions are very influential onto geometries of both pyranose rings (IdoA
12 and GlcNX) and the glycosidic linkage conformations between these residues.²⁴ The author
13 observed that the population of ¹C₄ chair conformation (Fig. 2) of the IdoA2S unit in heparin
14 disaccharides increases significantly in the presence of Ca²⁺ ions when compared to the same
15 structure in the presence of Na⁺ ions.
16
17
18
19
20
21
22
23

24 3. NMR-BASED DYNAMICS OF CHONDROITIN SULFATES: THE ROLE OF 25 OVERSULFATION AND TEMPERATURE 26

27
28 The single work describing NMR-based conformational fluctuations of chondroitin sulfates has
29 used chemical shift and scalar coupling constant values to examine the 3D-structural shapes of
30 chondroitin sulfate as a function of *O*-sulfonation levels and temperature.²⁷ After generating a
31 fully sulfated chondroitin sulfate by chemical reactions, the ¹H-NMR spectrum of this derivative,
32 at 30°C, showed that the composing GlcA units change their conformational preferences from
33 the usual ⁴C₁ chair conformer to the ¹C₄ chair conformer (Fig. 2). This conclusion was raised
34 primarily based on chemical shift and coupling constant changes upon conformational changes.
35 See that the ¹H resonances of the native chondroitin sulfate (Fig. 4A) go proportionally to
36 downfield regions upon partial *O*-sulfonation (Fig. 4B) and fully *O*-sulfonation (Fig. 4C). For
37 assignments of these peaks, see reference¹⁴. From Fig. 4C, we can also observe that at the fully
38 sulfated state, the splitting for coupling constants becomes of increased values; note that they are
39 now more evident for measurements at this bottom panel. Moreover, at 60°C the composing 2,6-
40 di-sulfated GlcA units of the oversulfated chondroitin sulfate can also exhibit the ²S₀ skew-boat
41 conformer (Fig. 2). This conclusion was raised again on the basis of conformational fluctuation-
42 induced changes of chemical shift (δ) and scalar coupling constant values of the GlcA from the
43 fully *O*-sulfonated chondroitin sulfate measured at 30 and 60°C temperatures (Table 1). This
44 reference work has clearly proven that unseen sugar ring conformations of composing units in
45 GAG polymers can become easily detectable when different sulfation patterns or higher
46 temperatures are taken into account. The ²S₀ conformer of chondroitin sulfate-composing GlcA
47 units becomes detectable due to the enhanced dynamical properties of this GAG type in solution
48 at conditions of high temperature combined with the oversulfated state.²⁷ Besides increasing the
49 sulfation content and thus electronegative charge density, the oversulfation reaction seems also
50
51
52
53
54
55
56
57
58
59
60

1
2
3 to enable conformational changes of the GlcA unit to a more biologically active form in terms of
4 anticoagulation.
5
6
7

8 9 **4. NMR-BASED DYNAMICS OF HYALURONAN: OLIGOSACCHARIDES AS** 10 **PRINCIPAL MODELS OF STUDY AND THE STRUCTURED BEHAVIOR IN** 11 **SOLUTION** 12

13
14 The aqueous solution conformational and dynamical properties of native hyaluronan have been
15 postulated to be very difficult to be examined because of the strong coupling and overlapping
16 resonances of this GAG type submitted to NMR spectroscopy analysis. This is likely because of
17 the simple structure of hyaluronan, which consequently gives rise to chemical shift degeneration
18 in its NMR spectrum,¹⁴ together with its common characteristics like high molecular weights,
19 low hydrosolubility mostly due to sulfation lack, and the well-structured behavior in solution.
20 Because of these factors, most of the studies concerning hyaluronan conformation and dynamics
21 are made on low molecular weight derivatives or short-, medium-sized oligosaccharides, usually
22 up to 12-mers, together with data analysis derived from NMR-restrained or unrestrained MD
23 simulations.
24
25
26
27

28 Proton-proton NOE NMR data combined with NMR-restrained MD data about dihedral
29 angles of a hyaluronan octasaccharide have been used in order to overcome the spectral
30 overlapping tendency of hyaluronan.²⁸ NMR-restrained MD calculations have yielded just one
31 set of interglycosidic dihedral angle values for the $\beta(1\rightarrow3)$ linkage (Fig. 1).²⁸ In contrast, two
32 sets of values were obtained for the $\beta(1\rightarrow4)$ linkage (Fig. 1), and these are consistent with the
33 experimental NOE-based data. The potential difference in flexibility derived from the two
34 glycosidic linkage types is consistent with both unrestrained and restrained MD trajectories
35 observed in the study.²⁸ The conformational and dynamical parameters of this reference were
36 used to predict a helical 3D-structural shape for the hyaluronan octasaccharide in solution. This
37 referential work has therefore clearly indicated a limited or restricted dynamical aspect of the
38 hyaluronan-derived octasaccharide due to the clear structured and rigid dynamic behavior of this
39 derivative in solution. These characteristics will be seen in the native hyaluronan molecule in
40 solution as discussed further.
41
42
43
44

45 Hyaluronan tetra- and hexasaccharides have been studied by a combination of
46 experimental and theoretical NMR data, complete relaxation matrix analysis, and MD
47 calculations.²⁹ Data based on rotation frame NOE, also known as ROE, have shown that both
48 $\beta(1\rightarrow3)$ and $\beta(1\rightarrow4)$ glycosidic linkages are rigid in solution. ROE is selectively obtained by
49 ROESY spectrum, which can be more successfully employed than NOESY in case of small
50 molecules, such as GAG short-oligosaccharides. Data based on ¹³C relaxation have shown a lack
51 of rotational degree of freedom of the hyaluronan hexasaccharide due to direct and/or water-
52 mediated inter-residue hydrogen bonding network collaborating to stabilize the oligosaccharide
53 structures in solution. Both single and tandem water bridges were found between the carboxylate
54 and the *N*-acetyl groups of these hyaluronan oligosaccharides. The carboxylate group of GlcA is
55
56
57
58
59
60

1
2
3 not involved in a direct link with the amide of the *N*-acetyl group of the GlcNAc unit, and this
4 was shown to facilitate the bonding network between the residues and water molecules. This
5 goes in favor with the structured property of the studied hyaluronan oligosaccharides and thus,
6 limited dynamic behavior of these molecules in solution.²⁹
7
8

9 In order to overcome the common resonance overlap in hyaluronan NMR studies, ¹⁵N
10 and ¹³C-isotopically labeled hyaluronan oligosaccharides (tetrasaccharides to dodecasaccharides)
11 were prepared and analyzed.³⁰ ¹⁵N-NMR spectra recorded for hyaluronan oligosaccharides with
12 lengths varying from 4- to 12-mers have shown that analysis based exclusively on the amide
13 groups of the composing GlcNAc units of hyaluronan allows spectral resolution and
14 interpretation of oligosaccharides up to 10-mers. In contrast, analysis based on ¹³C-natural
15 abundance allows resolution and interpretation on hyaluronan oligosaccharides up to 6-mers.
16 Complete ¹⁵N-based sequence-specific assignments of the hyaluronan oligosaccharides indicated
17 that chemical shift dispersion can be explained by end-effects, which are seen even in the middle
18 units of the 8-mers. The subtle chemical shift perturbations have suggested that different
19 conformations and dynamic process occur at the end of the hyaluronan oligosaccharides.³⁰ This
20 reference has inclusively raised hypothesis to explain the range of biological activities displayed
21 by the varying lengths of the hyaluronan derivatives based on enhanced dynamic behaviors of
22 the terminal units. This reference has clearly proven the advantage in using the ¹⁵N isotope for
23 achieving enough spectral resolution and assessing dynamic motions in hyaluronan derivatives.
24
25

26 A further work from the same group of the previous reference, and using the same
27 successful NMR approach based on ¹⁵N-NMR, now using ¹⁵N relaxation measurements on the
28 same ¹⁵N-labeled hyaluronan oligosaccharides (tetra-, hexa-, and octasaccharides), has enabled
29 extension of the background about the dynamical properties of hyaluronan oligosaccharides in
30 solution.³¹ The data interpretation based on ¹⁵N NOE enhancement and *T*₁ relaxation
31 measurements at three different magnetic fields (500, 600 and 750 MHz for proton Larmor
32 frequency) have pointed that while hyaluronan tetrasaccharides have a clear isotropic tumbling
33 behavior in solution, longer oligosaccharides are likely to exhibit a complex dynamic nature as
34 seen by the inconsistent fittings of their order parameters. The order parameters and motion
35 timescales obtained for the hyaluronan hexasaccharide were further converted into a quantitative
36 dynamic model as reproduced in Fig. 4. Based on this picture, besides the clear dynamical
37 process observed at the terminal units, also seen in the previous work,³⁰ the authors have
38 additionally shown that hyaluronan oligosaccharides can also exhibit substantial local
39 flexibilities. In this case, these internal motions can be seen by chemical side groups such as the
40 acetamido group, and by internal glycosidic linkages (Fig. 5).³¹ The latter, however, still limited
41 when compared to the glycosidic bonds of units located at the ends of the molecule (Fig. 4).
42
43

44 MD simulation-based conformational maps were used to achieve variations of the
45 dihedral angles in hyaluronan oligosaccharides, such as tetrasaccharides.³² ¹³C-NMR relaxation
46 data were also obtained to assess the dynamic chain patterns of this GAG as well as its low
47 molecular weight derivatives in solution.³² After scrutiny of several available force-fields, results
48 have shown substantial agreement between the native hyaluronan and oligomeric derivatives.
49
50
51
52
53
54
55
56
57
58
59
60

1
2
3 This implies that, hyaluronan oligosaccharides might have similar conformations and dynamic
4 properties in solution of the native molecule. This was also observed in the reference³¹, in which
5 the hyaluronan hexasaccharide starts to exhibit similar parameters of the native molecule in
6 solution.
7
8

9 A combination of NMR experimental and MD-based theoretical $^3J_{\text{H-H}}$ coupling constants
10 as well as NOE-related atomic distances associated with conformational plots for assessing
11 variations of the glycosidic dihedral angle values were all undertaken to examine the overall
12 conformational changes of hyaluronan oligosaccharides (tetra-, hexa-, and octasaccharides) in
13 solution.³³ Besides the clear motions at the terminal residues of both ends of the hyaluronan
14 molecules, and internal motions of the acetamido groups in middle residues, as represented with
15 the best structures obtained from the data (Fig. 6), the overall conformational shape observed for
16 the studied hyaluronan oligosaccharides in solution, especially the hexasaccharide, was the
17 contracted left-handed 4-fold helix. Generally, this is the 3D-structural arrangement widely
18 considered for hyaluronan molecules in solution. The results from this work are in total
19 agreement with previous reference.³¹
20
21
22
23

24 One of the single works describing NMR-based dynamic studies of native hyaluronan in
25 aqueous solution has used $^{13}\text{C-NMR}$ T_1 relaxation and NOE to assess conformational changes of
26 this high molecular weight GAG as a function of different temperatures (25, 35, 45, 55, 65, 75
27 and 85°C) and magnetic fields (300, 400, and 500 MHz for the proton Larmor frequency).³⁴ The
28 relaxation data have pointed segmental motions. Based on interpretation of the segmental
29 motions and amplitudes of librational motions of the C-H spin vectors at various carbon sites of
30 the hyaluronan composed sugar rings have led to the conclusion that intramolecular hydrogen
31 bonding of the stabilized secondary structure of hyaluronan plays a major role on the
32 conformational flexibility of this GAG in solution.³⁴
33
34
35
36
37
38

39 5. NMR/MD-BASED DYNAMICS OF THE GAG-COMPOSING N-ACETYLATED 40 AMINO SUGARS INDICATE RING CONFORMATIONAL CHANGES IN SOLUTION

41
42
43 The conformational changes of the *N*-acetylated amino sugars like α/β -GlcNX and α -GalNAc in
44 solution were examined through NMR- and MD-based $^3J_{\text{H-H}}$ coupling constant values.^{35,36}
45 Solvent effects as well as fittings using Karplus relationship were also considered in the
46 studies.^{35,36} The data have shown the following results. (i) The GlcNX unit is not a rigid $^4\text{C}_1$
47 chair (Fig. 2) conformer in solution.³⁶ This unit is able to undergo conformational changes when
48 free in solution according to polymerization degrees, *N*-substitutions and sulfation patterns. For
49 example, note the changes in the scalar coupling constant values according to *N*-substitutions and
50 sulfation patterns of the GlcNX units in aqueous solution as shown at Table 2. The *J* coupling
51 values were accurately measured by 900 MHz ^1H 1D NMR spectra.³⁶ (ii) The dynamical spread
52 of the acetamino group in free α -GlcNAc, β -GlcNAc, and α -GalNAc was measured as 32°, 42°,
53 and 20°, with corresponding mean dihedral angles of 160°, 180°, and 146°, respectively. This
54
55
56
57
58
59
60

1
2
3 indicates that anomericity as well as hydroxyl epimerization at the C4-position are sufficient to
4 cause changes on the global geometries of the GAG-composing amino sugars in solution. Hence,
5 even considering the same type of monosaccharide, in this case the *N*-acetylated amino sugars,
6 additional structural features are still relevant to modulate the overall conformation of these units
7 as well as their lateral chemical group (the acetamido group, for instance). The polymerization
8 degrees and additional substituents like *O*- and *N*-sulfonation have been also seen as important
9 determinants to the conformational and dynamical aspects of these GAG-composing amino
10 sugars free in solution.
11
12
13
14
15
16

17 6. CONCLUSIONS

18
19 The NMR-based dynamic studies of GAGs, derivatives or composing units free in solution have
20 used one or more of the following approaches: spin relaxation, scalar coupling constant and
21 chemical shift values, through-space NOE (ROE) resonances, combined or not with NMR-
22 restrained or unrestrained MD calculations. The most GAG types examined by NMR dynamics
23 are heparin, the structurally related heparan sulfate, chondroitin sulfate and hyaluronan.
24 Although the flexible IdoA (or IdoA2S) units in heparin and heparan sulfate chains is the
25 ultimate regulator for the conformational flexibility or dynamical properties of these GAGs in
26 solution, sulfation patterns are still the primary determinants of these properties. The 6-sulfation
27 seems to be the main contributor, but cooperative effects with *N*-sulfation were also observed.
28 Besides these intrinsic structural factors, extrinsic factors such as solvent, counterions and
29 temperature are also influential to dynamical process of these GAGs free in solution. Like for
30 heparin and heparan sulfate, the influences of sulfation patterns, especially oversulfation, and
31 high temperatures were also observed to be clear contributors to the conformational changes of
32 the composing units in chondroitin sulfate chains. In hyaluronan, the high tendency of NMR
33 spectral overlapping occasioned by the simple structure and lack of sulfation associated with
34 common structural features like high molecular weight, low hydrosolubility and dynamics has
35 made hyaluronan the most difficult GAG type for NMR dynamic analysis. In order to overcome
36 some obstacles, the majority of the NMR studies have used hyaluronan-derived oligosaccharides
37 together with MD analysis. In general, the main conclusions from the several works are in fine
38 agreement. The conclusions are in favor with a very structured and limited dynamic behavior of
39 the medium-sized hyaluronan oligosaccharides in solution, as seen for the native hyaluronan
40 molecule. In fact, a dominant contracted left-handed fourfold helical shape has been shown for
41 hyaluronan, and its medium-sized derived oligosaccharides in solution. The composing GAG
42 units like the *N*-acetyl amino sugars like differentially substituted glucosamines, α -GlcNAc, β -
43 GlcNAc, and α -GalNAc were also studied regarding their dynamical properties, and results have
44 led the conception that slight structural changes in these monosaccharides, like sulfation patterns,
45 the C4-epimerization and anomericity are enough to cause shift on their ring conformation
46 distribution.
47
48
49
50
51
52
53
54
55
56
57
58
59
60

Conflict of interest

The author states that he is not aware of any authorship, affiliations, memberships, funding, or financial holdings that might be perceived as damaged or as affecting the objectivity of the content of this material. The author declares no conflict of interest by any part. The reprint of figures in this review was obtained from the published materials under copyright and license agreement.

Funding

This study was supported by the grants Universal-14/2013-[470330/2013-9] and E-26/110.961/2013 from Conselho Nacional de Desenvolvimento Científico e Tecnológico (CNPq) and Fundação de Amparo à Pesquisa do Estado do Rio de Janeiro (FAPERJ), respectively. The content of this work is solely the responsibility of the author and does not necessarily represent the official views of the funding agencies.

References

- 1 D.L. Rabenstein, Heparin and heparan sulfate: structure and function, *Nat. Prod. Rep.* 2002, **19**(3), 312-331.
- 2 R. Sasisekharan, G. Venkataraman, Heparin and heparan sulfate: biosynthesis, structure and function, *Curr. Opin. Chem. Biol.*, 2000, **4**(6), 626-631.
- 3 K. Sugahara, H. Kitagawa, Heparin and heparan sulfate biosynthesis, 2002, *IUBMB Life*, **54**(4), 163-175.
- 4 K. Sugahara, T. Mikami, T. Uyama, S. Mizuguchi, K. Nomura, H. Kitagawa, Recent advances in the structural biology of chondroitin sulfate and dermatan sulfate. *Curr. Opin. Struct. Biol.*, 2003, **13**(5), 612-620.
- 5 A. Almond, Hyaluronan, *Cell Mol. Life Sci.*, 2007, **64**(13), 1591-1596.
- 6 V.H. Pomin, Solution NMR conformation of glycosaminoglycans, *Prog. Biophys. Mol. Biol.* 2014, **114**(2), 61-68.
- 7 R. Raman, G. Venkataraman, S. Ernst, V. Sasisekharan, R. Sasisekharan, Structural specificity of heparin binding in the fibroblast growth factor family of proteins, *Proc. Nat. Acad. Sci.*, 2003, **100**(5), 2357-2362
- 8 L. Nieto, A. Canales, I.S. Fernández, E. Santillana, R. González-Corrochano, M. Redondo-Horcajo, F.J. Cañada, P. Nieto, M. Martín-Lomas, G. Giménez-Gallego, J. Jiménez-Barbero, Heparin modulates the mitogenic activity of fibroblast growth factor by inducing dimerization of its receptor. A 3D view by using NMR, *Chembiochem*, 2013, **14**(14), 1732-1744.
- 9 T.R. Rudd, M.A. Skidmore, M. Guerrini, M. Hricovini, A.K. Powell, G. Siligard, E.A. Yates, The conformation and structure of GAGs: recent progress and perspectives, *Curr. Opin. Struct. Biol.*, 2010, **20**(5), 567-574.

- 10 M.F. García-Mayoral, A. Canales, D. Díaz, J. López-Prados, M. Moussaoui, J.L. de Paz, J. Angulo, P.M. Nieto, J. Jiménez-Barbero, E. Boix, M. Bruix, Insights into the glycosaminoglycan-mediated cytotoxic mechanism of eosinophil cationic protein revealed by NMR, *Glycobiol.*, 2012, **8**(1), 144-151.
- 11 T. Reddy, J.K. Rainey, Interpretation of biomolecular NMR spin relaxation parameters, *Biochem. Cell. Biol.*, 2010, **88**(2), 131-142.
- 12 K. Li, Z. Zu, J. Xu, V.A. Janve, J.C. Gore, M.D. Does, D.F. Gochberg, Optimized inversion recovery sequences for quantitative T1 and magnetization transfer imaging, *Magn. Reson. Med.*, 2010, **64**(2), 491-500.
- 13 I.R. Kleckner, M.P. Foster, An introduction to NMR-based approaches for measuring protein dynamics, *Biochim. Biophys. Acta*, **1814**(8), 942-968.
- 14 V.H. Pomin, NMR chemical shifts in structural biology of glycosaminoglycans, *Anal. Chem.*, 2014, **86**(1), 65-94.
- 15 E. Fadda, R.J. Woods, Molecular simulations of carbohydrates and protein-carbohydrate interactions: motivation, issues and prospects. *Drug Discov. Today*, **15**(15-16), 596-609.
- 16 R.J. Woods, M.B. Tessier, Computational glycoscience: characterizing the spatial and temporal properties of glycans and glycan-protein complexes, *Curr. Opin. Struct. Biol.*, 2010, **20**(5), 575-583.
- 17 M. Karplus, Contact Electron-Spin Coupling of Nuclear Magnetic Moments. *J. Chem. Phys.*, 1959, **30**(1), 11-15.
- 18 M. Karplus, Vicinal Proton Coupling in Nuclear Magnetic Resonance. *J. Am. Chem. Soc.*, 1963, **85**(18), 2870-2871.
- 19 B. Mulloy, M. Forster, Conformation and dynamics of heparin and heparan sulfate, *Glycobiol.*, 2000, **10**(11), 1147-1156.
- 20 M. Mobli, M. Nilsson, A. Almond, The structural plasticity of heparan sulfate NA-domains and hence their role in mediating multivalent interactions is confirmed by high-accuracy ¹⁵N-NMR relaxation studies, *Glycoconj. J.*, 2008, **25**(5), 401-414.
- 21 M. Hricovíni, G. Torri, Dynamics in aqueous solutions of the pentasaccharide corresponding to the binding site of heparin for antithrombin III studied by NMR relaxation measurements, *Carbohydr. Res.* 1995, **268**(2), 159-175.
- 22 J. Angulo, M. Hricovíni, M. Gairi, M. Guerrini, J.L. de Paz, R. Ojeda, M. Martín-Lomas, P. M. Nieto, Dynamic properties of biologically active synthetic heparin-like hexasaccharides, *Glycobiol.* 2005, **15**(10), 1008-1015.
- 23 K.J. Murphy, N. McLay, D.A. Pye, Structural studies of heparan sulfate hexasaccharides: new insights into iduronate conformational behavior, *J. Am. Chem. Soc.*, 2008, **130**(37), 12435-12444.
- 24 M. Hricovíni, Effect solvent and counterions upon structure and NMR spin-spin coupling constants in heparin disaccharide, *J. Phys. Chem. B.*, 2011, **115**(6), 1503-1511.
- 25 B. Mulloy, M.J. Forster, C. Jones, D.B. Davies, N.m.r. and molecular-modelling studies of the solution conformation of heparin, *Biochem. J.*, 1993, **293**(Pt3), 849-858.

- 1
2
3
4
5
6
7
8
9
10
11
12
13
14
15
16
17
18
19
20
21
22
23
24
25
26
27
28
29
30
31
32
33
34
35
36
37
38
39
40
41
42
43
44
45
46
47
48
49
50
51
52
53
54
55
56
57
58
59
60
- 26 B. Mulloy, M.J. Forster, C. Jones, A.F. Drake, E.A. Johnson, D.B. Davies, The effect of variation of substitution on the solution conformation of heparin: a spectroscopic and molecular modelling study, *Carbohydr. Res.*, 1994, **255**, 1-26.
- 27 T. Maruyama, T. Toida, T. Imanari, G. Yu, R.J. Linhardt, Conformational changes and anticoagulant activity of chondroitin sulfate following its *O*-sulfonation, *Carbohydr. Res.*, 1998, **306**(1-2), 35-43.
- 28 S. M. A. Holmbeck, P. A. Petillo, L. E. Lerner, The solution conformation of hyaluronan: a combined NMR and molecular dynamics study, *Biochem.*, 1994, **33**(47), 14246-14255.
- 29 A. Donati, A. Magnani, C. Bonechi, R. Barbucci, C. Rossi, Solution structure of hyaluronic acid oligomers by experimental and theoretical NMR, and molecular dynamics simulation, *Biopol.*, 2001, **59**(6), 434-445.
- 30 C. D. Blundell, P. L. DeAngelis, A. J. Day, A. Almond, Use of ¹⁵N-NMR to resolve molecular details in isotopically-enriched carbohydrates: sequence-specific observations in hyaluronan oligomers up to decasaccharides, *Glycobiol.*, 2004, **14**(11), 999-1009.
- 31 A. Almond, P. L. DeAngelis, C. D. Blundell, Dynamics of hyaluronan oligosaccharides revealed by ¹⁵N relaxation, *J. Am. Chem. Soc.*, 2005, **127**(4), 1086-1087.
- 32 S. Furlan, G. L. Penna, A. Perico, A. Cesàro, Hyaluronan chain conformation and dynamics, *Carbohydr. Res.*, 2005, **340**(5), 959-970.
- 33 A. Almond, P. L. DeAngelis, C. D. Blundell, Hyaluronan: the local solution conformation determined by NMR and computer modeling is close to a contracted left-handed 4-fold helix, *J. Mol. Biol.*, 2006, **358**(5), 1256-1269.
- 34 P. Dais, E. Tyliaakis, J. Kanetakis, F. R. Taravel, ¹³C nuclear magnetic relaxation study of segmental dynamics of hyaluronan in aqueous solution, *Biomacromol.*, 2005, **6**(3), 1397-1404.
- 35 M. Mobli, A. Almond, *N*-acetylated amino sugars: the dependence of NMR ³J_(HN-H2)-couplings on conformation, dynamics and solvent, *Org. Biomol. Chem.*, 2007, **5**(14), 2243-2251.
- 36 B. M. Sattelle, A. Almond, Is *N*-acetyl-D-glucosamine a rigid ⁴C₁ chair?, *Glycobiol.*, 2011, **21**(12), 1651-1662.
- 37 M. Hricovíni, F. Bizik, Relationship between structure and three-bond proton-proton coupling constants in glycosaminoglycans, *Carbohydr. Res.*, 2007, **342**(6), 779-783.
- 38 C. Altona, C.A.G. Haasnoot, Prediction of anti and gauche vicinal proton-proton coupling constants in carbohydrates: A simple additivity rule for pyranose rings, *Org. Magn. Reson.* 1980, **13**(6), 417-429.
- 39 M. Mobli, A. Almond, *N*-Acetylated amino sugars: The dependence of NMR 3J(HNH2)-couplings on conformation, dynamics and solvent, *Org. Biomol. Chem.* 2007, **5**(14), 2243-2251.
- 40 C.D. Blundell, I.S. Roberts, J.K. Sheehan, A. Almond, Investigating the molecular basis for the virulence of *Escherichia coli* K5 by nuclear magnetic resonance analysis of the capsule polysaccharide, *J. Mol. Microbiol. Biotechnol.* 2009, **17**(2), 71-82.

Tables**Table 1** Conformational fluctuation-induced chemical shift (δ , in ppm) and scalar coupling constant changes (in Hz) of the composing residues of a fully *O*-sulfonated chondroitin sulfate analyzed by NMR at 30 and 60°C. Modified with permission.¹⁷

Residue (temperature)	(δ)	(δ)	(δ)	(δ)	(δ)
	J_{H1-H2}	J_{H2-H3}	J_{H3-H4}	J_{H4-H5}	J_{H5-H6}
GalNAc (30°C)	(4.88)	(4.11)	(4.11)	(5.02)	(4.05)
	7.82	nd ^a	nd	<1.5	6.1
GalNAc (60°C)	(4.86)	(4.10)	(4.10)	(5.02)	(4.06)
	7.4	nd	nd	<1.5	6.2
GlcA (30°C)	(5.00)	(4.59)	(4.94)	(4.59)	(4.23)
	5.9	nd	<1.5	<1.5	
GlcA (60°C)	(4.97)	(4.53)	(4.94)	(4.55)	(4.20)
	<1.5	<1.5	<1.5		

^a Not determined.

Table 2 Observed (Obs.) and calculated (Calc.) $^3J_{\text{H-H}}$ (Hz) for the five differently substituted α -D-glucosamine types in water. Modified with permission from reference³⁶.

Hexosamine	Coupling	Obs.	Calc.
GlcNAc	$J_{\text{H1-H2}}$	3.5	3.2
GlcNAc	$J_{\text{H2-H3}}$	10.7	10.1
GlcNAc	$J_{\text{H3-H4}}$	9.9	9.9
GlcNAc	$J_{\text{H4-H5}}$	9.3	10.0
GlcNAc	$J_{\text{HN-H2}}$	8.8	9.7
GlcNAc	$J_{\text{H5-H6R}}$	5.2 ^a	4.5
GlcNAc	$J_{\text{H5-H6S}}$	2.3 ^a	3.2
GlcNS	$J_{\text{H1-H2}}$	3.5	2.6
GlcNS	$J_{\text{H2-H3}}$	10.4	10.2
GlcNS	$J_{\text{H3-H4}}$	9.0	9.9
GlcNS	$J_{\text{H4-H5}}$	10.2	10.0
GlcNS6S	$J_{\text{H1-H2}}$	3.5	2.6
GlcNS6S	$J_{\text{H2-H3}}$	10.4	8.8
GlcNS6S	$J_{\text{H3-H4}}$	9.1	9.8
GlcNS6S	$J_{\text{H4-H5}}$	10.1	9.9
GlcNS6S3S	$J_{\text{H1-H2}}$	3.3	2.7
GlcNS6S3S	$J_{\text{H2-H3}}$	10.7	10.2
GlcNS6S3S	$J_{\text{H3-H4}}$	8.9	8.3
GlcNS6S3S	$J_{\text{H4-H5}}$	10.1	10.0
GlcNS3S	$J_{\text{H1-H2}}$	3.3	2.7
GlcNS3S	$J_{\text{H2-H3}}$	10.7	10.2
GlcNS3S	$J_{\text{H3-H4}}$	8.8	9.9
GlcNS3S	$J_{\text{H4-H5}}$	10.1	8.5

The Karplus equations used to derive the values obtained in this table were used based on references³⁷⁻³⁹. Experimental errors were estimated to be ± 0.2 Hz and standard deviations of calculated ring vicinal couplings were estimated to be at most 0.01 Hz. (except GlcNAc $J_{\text{H5-H6R}}$ which was ± 0.1 Hz). ^aData from a previous NMR study.⁴⁰

Figure Legends

Fig. 1 Representative structures of the GAG types mostly studied by NMR dynamics.

Fig. 2 Structural representation of the sugar ring conformations (chairs, C, and skew-boat, S) of the α -IdoA unit, seen in certain GAG types such as heparin and heparan sulfate, taken here as structural model for the nomenclatures 4C_1 , 1C_4 and 2S_0 . Carbon atoms are numbered accordingly to their positions within the sugar ring.

Fig. 3 Diagrams of the solution conformations obtained for the studied heparin structure 1, an unmodified dodecasaccharide (A and B) with the composing IdoA unit in its 1C_4 chair (A) or in its 2S_0 skew-boat conformer (B), and for the studied heparin structure 2, a fully desulfated re-*N*-acetylated dodecasaccharide (C and D) with the composing IdoA unit in its 1C_4 chair (C) or in its 2S_0 skew-boat conformer (D). In panels A and B, sulfate and carboxylate groups are respectively marked by solid lines or asterisks. A2, I2 and A6 denote sulfations at 2-positions of the glucosamine, iduronic acid, and 6-position of glucosamine. See slight differences between panels A versus B, C versus D, but more noticeable differences between A versus C, and B versus D. Data modified with permission.^{25,26}

Fig. 4 1H 1D NMR spectra of chondroitin sulfate and chemically *O*-sulfonated chondroitin sulfates measured at 30°C. (A) Intact bovine tracheal chondroitin sulfate. (B) Partially *O*-sulfonated chondroitin sulfate prepared from bovine tracheal chondroitin sulfate. (C) Fully *O*-sulfonated chondroitin sulfate. Modified with permission.¹⁷

Fig. 5 Set of 20 structures obtained by overlaying the central two sugars in the hyaluronan hexasaccharide studied in reference³¹. The amide conformational spread, as observed by ${}^{15}N$ resonances, is due to (A) deviations of the glycosidic linkages, and (B) acetamido libration. Reprinted with permission from³¹. Copyright 2014 American Chemical Society.

Fig. 6 Overlays of 40 structures obtained from the NMR-MD combined study on hyaluronan (A) tetrasaccharide, (B) hexasaccharide, and (D) octasaccharide. (C) Represents the structures considering the NMR data only. See the similarity between panels (B) and (C) for data validation. Reproduced from³³ with permission.

Figures

Figure 1

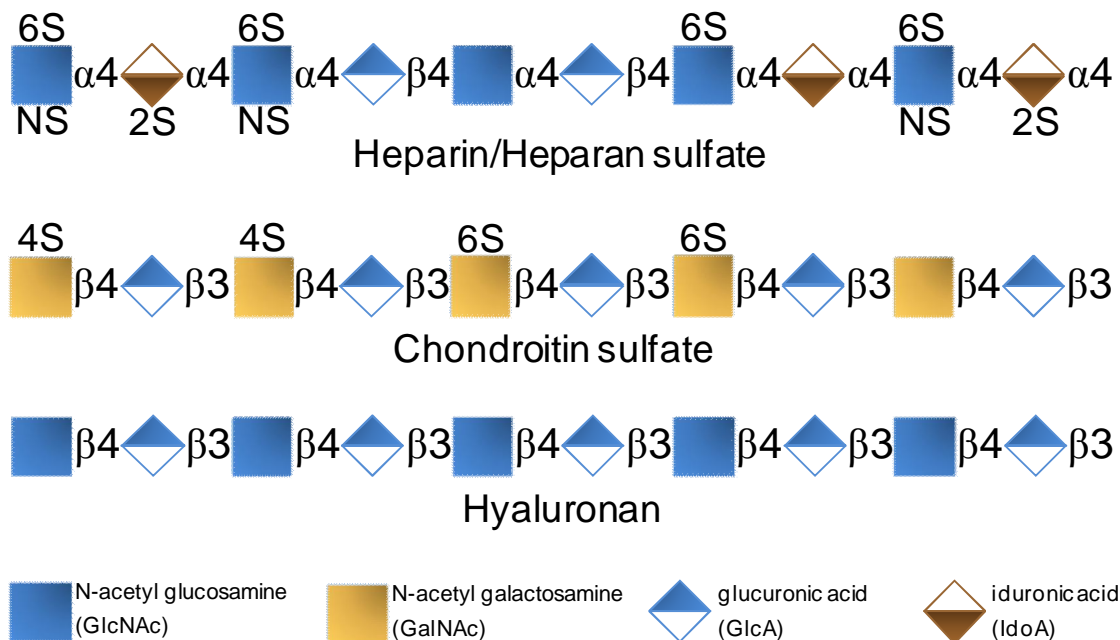
1
2
3
4
5
6
7
8
9
10
11
12
13
14
15
16
17
18
19
20
21
22
23
24
25
26
27
28
29
30
31
32
33
34
35
36
37
38
39
40
41
42
43
44
45
46
47
48
49
50
51
52
53
54
55
56
57
58
59
60

Figure 2

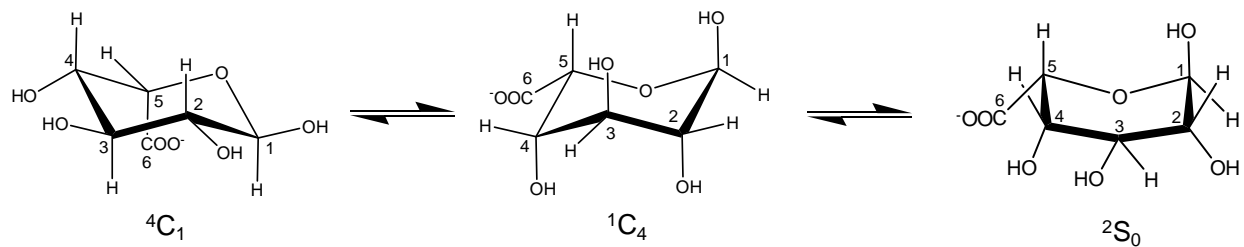
1
2
3
4
5
6
7
8
9
10
11
12
13
14
15
16
17
18
19
20
21
22
23
24
25
26
27
28
29
30
31
32
33
34
35
36
37
38
39
40
41
42
43
44
45
46
47
48
49
50
51
52
53
54
55
56
57
58
59
60

Figure 3

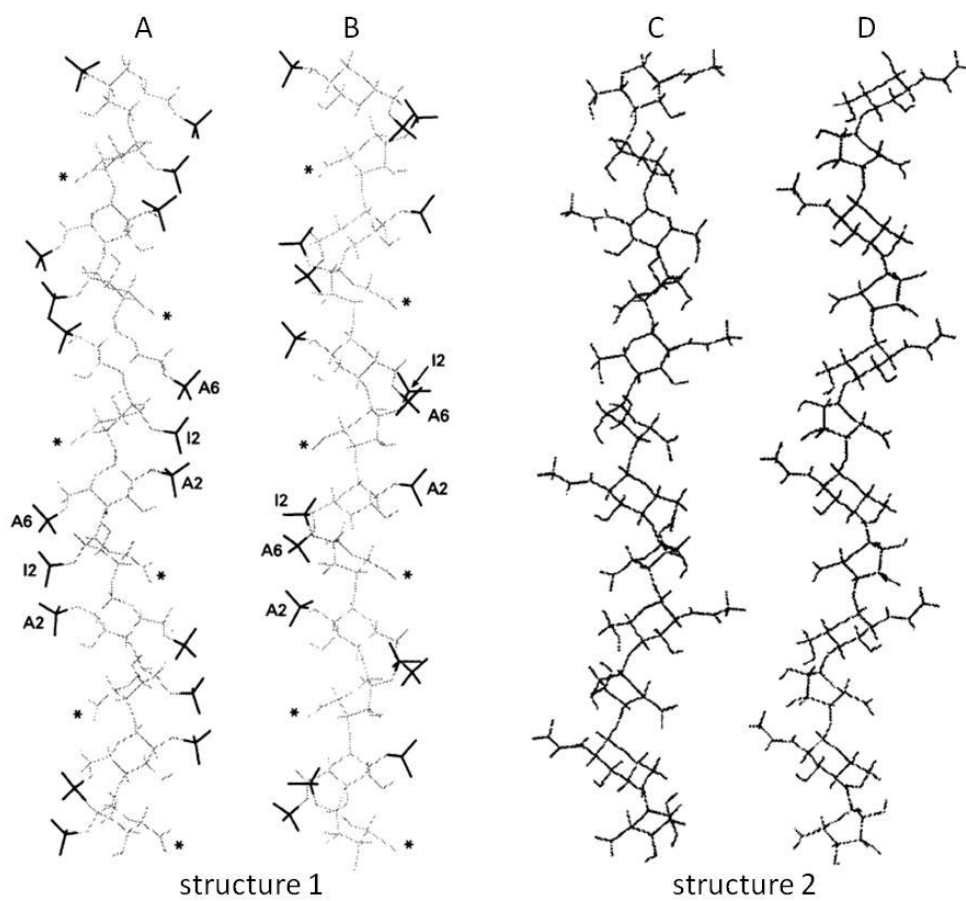
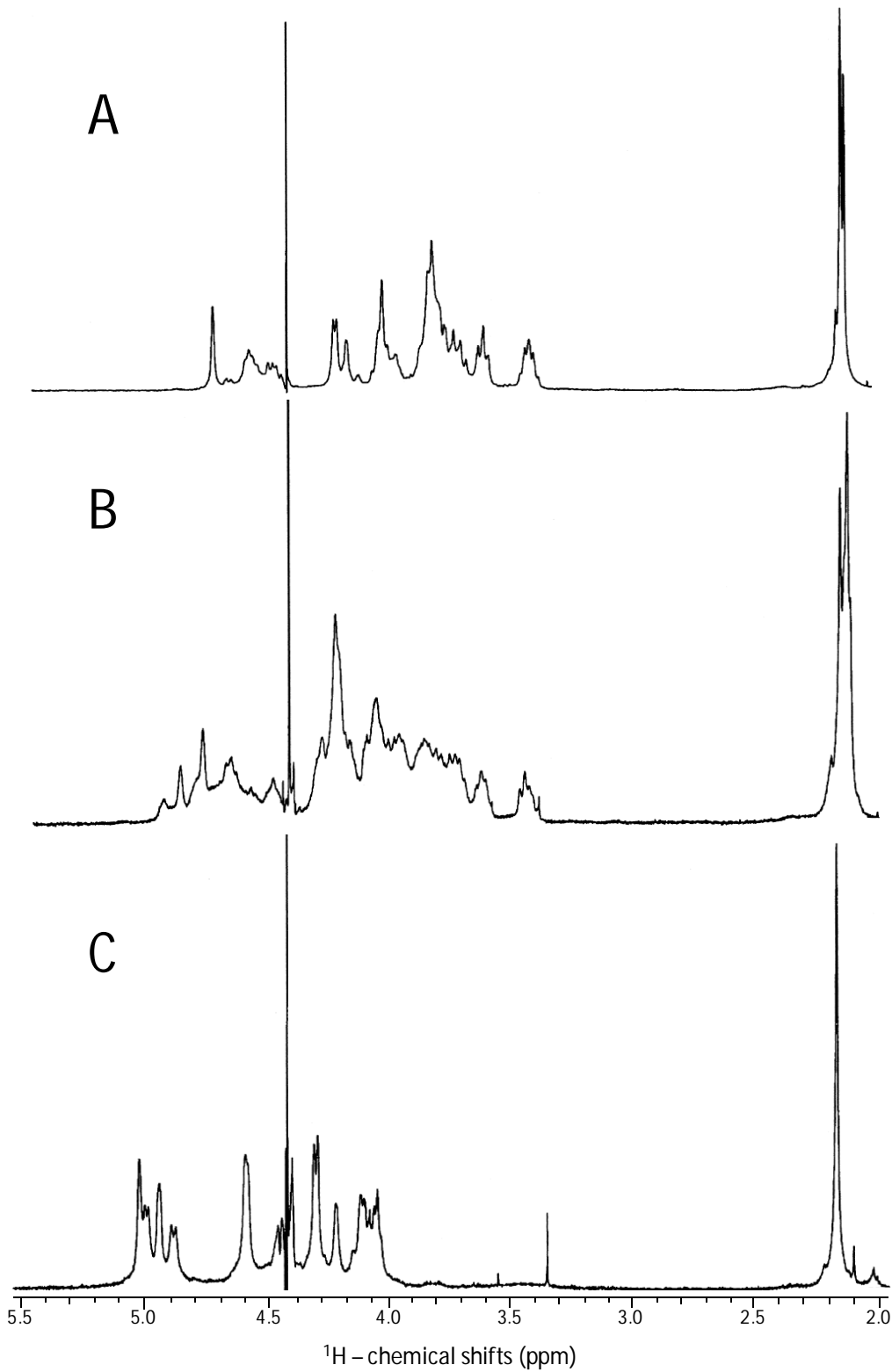


Figure 4



1
2
3
4
5
6
7
8
9
10
11
12
13
14
15
16
17
18
19
20
21
22
23
24
25
26
27
28
29
30
31
32
33
34
35
36
37
38
39
40
41
42
43
44
45
46
47
48
49
50
51
52
53
54
55
56
57
58
59
60

Figure 5

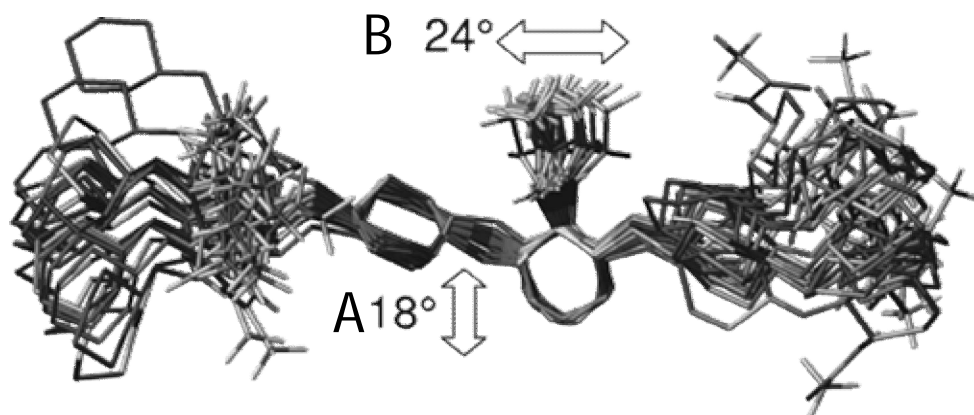
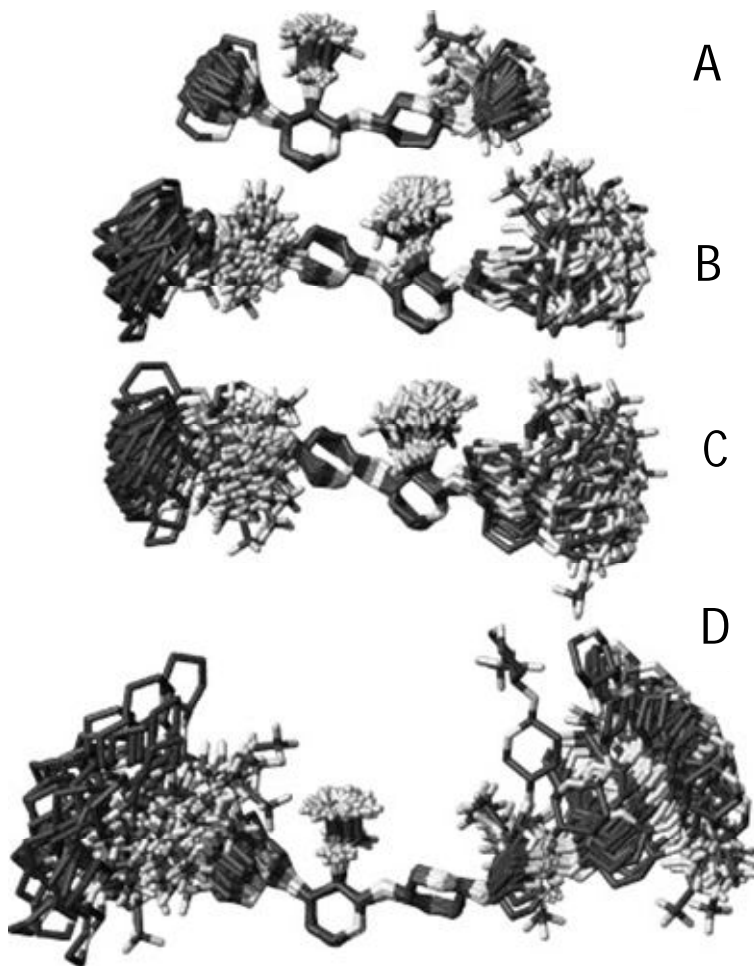
1
2
3
4
5
6
7
8
9
10
11
12
13
14
15
16
17
18
19
20
21
22
23
24
25
26
27
28
29
30
31
32
33
34
35
36
37
38
39
40
41
42
43
44
45
46
47
48
49
50
51
52
53
54
55
56
57
58
59
60

Figure 6



1
2
3
4
5
6
7
8
9
10
11
12
13
14
15
16
17
18
19
20
21
22
23
24
25
26
27
28
29
30
31
32
33
34
35
36
37
38
39
40
41
42
43
44
45
46
47
48
49
50
51
52
53
54
55
56
57
58
59
60



Dynamical behaviors of glycosaminoglycans, as here illustrated with a hyaluronan oligosaccharide, are key regulators to their biological functions.

62x25mm (96 x 96 DPI)

1
2
3
4
5
6
7
8
9
10
11
12
13
14
15
16
17
18
19
20
21
22
23
24
25
26
27
28
29
30
31
32
33
34
35
36
37
38
39
40
41
42
43
44
45
46
47
48
49
50
51
52
53
54
55
56
57
58
59
60